# Evaluating the Sim-to-Real Gap for Contact-Rich Robotic Manipulation Tasks using Suction Cups

Maarten Johannes Jongeneel, Alexander Oliva, Fredrik Nordfeldth, Ricardo Duarte, Steven Eisinger, Heico Sandee, Claude Lacoursière, Alessandro Saccon

# Evaluating the Sim-to-Real Gap for Contact-Rich Robotic Manipulation Tasks using Suction Cups

M.J. Jongeneel[1], A.A. Oliva[1], F. Nordfeldth[2], R. Duarte[3], S. Eisinger[3], H Sandee[3], C. Lacoursière[1,2], and A. Saccon[1]

***Abstract*— Despite the wide adoption of suction cups in automated logistic processes, their usage for contact-rich manipulation tasks is limited. This limitation is due to unpredictable large deformations of the suction cup that can arise in contact-rich tasks, making motion planning an unsolved problem. A scenario in which these type of motions occur is in bin-packing. Allowing a robot to push or squeeze items into tight spaces would increase considerably the achievable packing density of current industrial bin-packing solutions, with important economic and environmental benefits. To enable robotic systems to perform these motions, we first integrate a newly developed compact 6D suction cup model into a physics engine. We subsequently evaluate the sim-to-real gap by evaluating object-pose and force/torque predictions for contact-rich manipulation tasks against experiments where object motions are tracked with an accurate motion capture system and interaction forces are recorded by means of a force/torque sensor mounted on the tool arm. We show that, by the chosen physics engine and the suction cup model, these simulations can lead to high prediction accuracy, even for large deformations of the suction cup up to 30 degrees. By combining these simulations with sufficiently intelligent motion and packing algorithms, packing density performance far superior to the current state of the art and comparable to human operators can be achieved.**

## I. Introduction

In logistics bin-packing scenarios, tight placement of objects into containers is essential to reach high stacking densities in order fulfillment [1]. In current industrial applications, these tasks are still completed by a large number of manual workers [2], [3]. However, the rapid development of e-commerce and labor scarcity have attracted much interest in developing automated solutions for these logistic tasks. The bin-packing problem (BPP), which covers the study of automating these logistic tasks, is widely studied in literature [3]–[8], and aims to optimize this process by minimizing the number of containers used or maximizing the space utilization within a container. Although some works consider grippers with fingers [3], [6], most works employ a suction-based vacuum gripper as they are capable of handling a wide variety of objects [9], [10]. These suction cups can also be used as compliant parts, allowing for contact-rich manipulation to increase packing density [4], [7], see also Figure 1. Despite the large industrial interest, however, the literature on contact-rich manipulation tasks using suction cups is rather limited. Works that do consider the exploitation of contacts for the bin-packing problem (e.g., by pushing or tilting) typically limit the motions of the robot to those where small deformations of the suction cup occur [4], [11]. This is because large deformations of the suction cup are hard to predict while required for motion planning of these advanced tasks [12]. Multiple modeling attempts have been made [13], [14], but estimating the object pose from these models can still lead to large errors [13] or inaccurate predictions when large torques are applied [14]. Additionally, and to the best of the author's knowledge, there does not exist work focusing on the validation of suction-cup models in the context of contact-rich manipulation tasks, where large deformations of the suction cup are expected. Therefore, in this work, we will employ a compact 6D suction cup model [12] that provides accurate object-pose and force/torque estimations for large deformations, and that was recently developed to this end by some of the authors of this paper. We incorporate this model in the AGX Dynamics physics engine [15] due to its known fidelity and numerical stability in challenging contact scenarios, and employ this simulation environment to create a stacking pattern for the bin-packing problem. We validate the simulations on an experimental setup mimicking the simulation environment, both using the same controller, showing accurate predictions of the object pose and force/torque predictions during advanced manipulation tasks. In summary, the main contributions are:

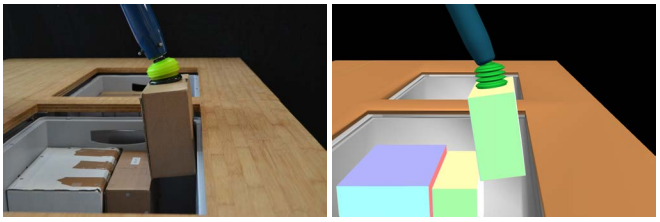

Fig. 1: Example of a bin-packing scenario. Note how the deformation of the suction cup in experiments (left) is closely captured in simulation (right). (The mesh deformation in simulation is graphically not rendered).

- Integration of the suction-cup model [12] in a multi-body dynamics physics engine;
- Validation of this model in the context of contact-rich manipulation tasks for the bin-packing problem;
- Sharing of a dataset containing experiments with object and robot motions and interaction force recordings of 5 different stacking patterns with 18 different boxes;

Besides this introduction, this paper has the following structure. In Section II, we specify the scenario and objectives. In Section III, we subsequently provide an overview of the

[1]M.J. Jongeneel, A.A. Oliva, C. Lacoursière, and A.Saccon are with the Faculty of Mechanical Engineering, Eindhoven University of Technology (TU/e), The Netherlands (*M.J. Jongeneel and A.A. Oliva are co-first authors*) (*Corresponding author: M.J. Jongeneel*) {m.j.jongeneel, a.a.oliva, c.lacoursiere, a.saccon}@tue.nl

[2]F. Nordfeldt and C. Lacoursière are with Algoryx Simulation AB {fredrik.nordfeldth, claude.lacoursiere}@algoryx.com

[3]S. Eisinger, R. Duarte and H. Sandee are with SmartRobotics {seisinger, rduarte, hsandee}@smart-robotics.nl

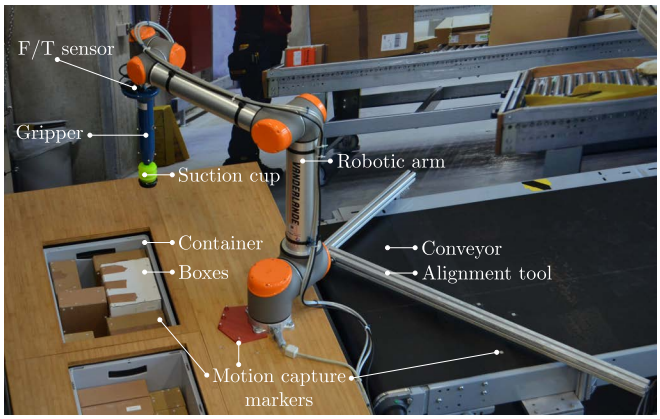


Fig. 2: The experimental setup with the various components indicated.

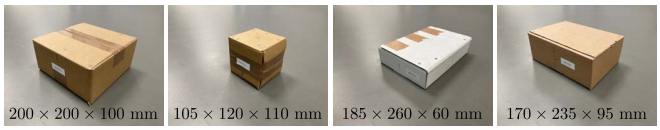


Fig. 3: Four different type of boxes used in the experiments.

framework, including the simulation environment, the control framework with trajectory planning, the robot model, the environment modeling, contact description, and the motion primitives. In Section IV, we describe the experimental setup and data collection procedure, while in Section V, we analyze the experimental results and evaluate the sim-to-real gap considering the prediction of the object pose and forces/torques acting on the gripper. Finally, Section VI covers the conclusion and recommendations for future work.

## II. Scenario Specification

We consider the scenario of fulfillment orders in a warehouse by a robotic arm, as depicted in Figure 2. In this scenario, the robot picks items arriving in a particular sequence from a pick location and places them in a target container. The objective is to fill the container as much as possible, thereby achieving a certain *packing density*, which we define as the ratio between the total volume of the items in the container and the volume of the container itself.

In our case, we define the pick location by a metal frame placed on the conveyor, also depicted in Figure 2. The robotic arm (UR10), attached vacuum gripper with the suction cup, conveyor, and workbench with container together represent the type and size used in warehousing systems where pick-and-place robotic solutions operate. We will provide additional details about the setup in Section IV. The items' properties are based on industry data, resulting in *item sets*, and the *item sequences* define the order in which they arrive in the system. We detail the item sets and sequences below, where we consider five different item sequences with a total of 18 different boxes.

**Item sets:** To evaluate the performance of bin-packing in realistic and industry-relevant settings, the item set and packing orders used in the test scenario are based on real-world data of items packed by robots at customer sites of two logistics companies. For the sake of simplicity, we consider

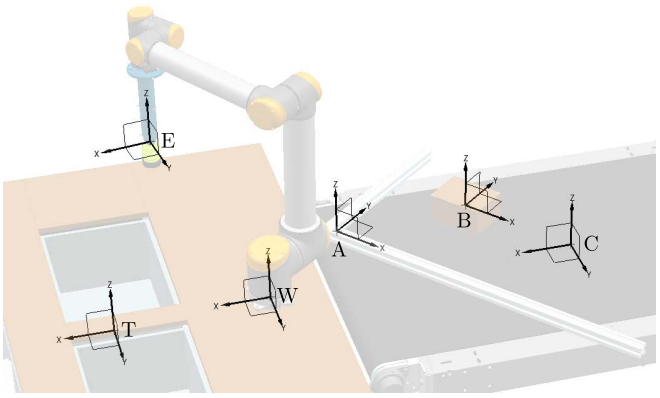


Fig. 4: The simulation environment with indication of the frames.

carton boxes only. We created 18 carton boxes based on the four most frequent representative dimensions in the parcel industry[1] as displayed in Figure 3. These boxes are all tightly filled (to avoid movable parts) with different materials to allow for controlled experiments, resulting in object masses ranging from 250g to 1.050kg, where some boxes have an off-centered center of mass. Additional details are in the dataset provided adjacent to this publication and on the impact-aware-robotics-database website [16].

**Item sequence:** An item sequence is defined as the order in which items reach the robot. To mimic an automated warehouse system, they arrive in a random order, independent of the container's content, requiring the robot to decide ad-hoc on placement. We generated five different item sequences using the four base items shown in Figure 3. These sequences approximate real-world scenarios where multiple instances of a particular item are requested in succession. Furthermore, they have the minimum number of boxes required to reach a theoretical maximum filling degree (packing density) of 90%, given the box and container dimensions.

## III. Framework Description

Since online task and motion planning in contact-rich applications employing suction cups is still an open problem [17], we will make use of the simulation environment to manually create the stacking patterns. Potential online task-and-motion planners can be based on sampling-based MPC or RL approaches that include contact interactions explicitly and are, potentially, capable of quickly replanning in the presence of failure [18], [19]. We envision the model-based approach presented in this work as part of the solution, assuming it provides accurate force and motion predictions. In this paper, our goal is to quantify the discrepancies between simulations and experiments in the object handling context.

**Simulation environment:** Figure 4 schematically shows the simulated setup, including the different reference frames.

[1]This follows from an internal discussion with Vanderlande, a global partner for logistic process automation. See also `https://www.vanderlande.com/`

TABLE I: Contact parameters used in the simulation environment.

| Object 1 | Object 2 | Friction $\mu$ | Restitution $e_N$ |
|---|---|---|---|
| Box | Box | 0.2 | 0.05 |
| Box | Container | 0.24 | 0.1 |
| Box | Workbench | 0.15 | 0.1 |

Frame $A$ defines the alignment tool, which defines the pick-up position and orientation of the boxes. Frame $E$ defines the control point of the robotic arm. Frame $W$ is located at the robot origin and used as the world frame. Frame $C$ defines the conveyor, and frame $T$ defines the container. Given the world frame $W$, we express the poses of the alignment tool, the container, and the conveyor with transformation matrices according to the notation as in [20]. For example, we express the relative orientation and position of frame $A$ with respect to frame $W$ according to

$$ {}^{W}\mathbf{H}_{A} = \begin{bmatrix} {}^{W}\mathbf{R}_{A} & {}^{W}\mathbf{o}_{A} \\ \mathbf{0}_{1\times 3} & 1 \end{bmatrix}, \tag{1} $$

where ${}^{W}\mathbf{R}_{A} \in \mathrm{SO}(3)$ is the rotation matrix from $A$ to $W$ and ${}^{W}\mathbf{o}_{A} \in \mathbb{R}^3$ is the position of frame $A$ with respect to frame $W$. These transformations are measured in the lab to replicate the setup as closely as possible.

We employ the RACK simulation framework with AGX Dynamics [15] as the physics engine for the simulation environment. RACK is a simulation framework explained in [21] and developed in collaboration with Algoryx and CNRS-AIST JRL within the European project on Impact-Aware Manipulation[2]. It is publicly available[3], which means the results presented in this work can straightforwardly be reproduced, both in simulation and experiment and we consider this work as a first example using this framework. It uses a human-readable language called BRICK to set up the simulation scene and allows for simulations with synchronous robot control through a communication protocol called CLICK [21]. AGX Dynamics has been developed since 2007 and is used widely by engineering firms[4] and recently also gaining interest in academia [22]–[26], with a possibility for free trial licenses[5]. The theory behind this software is explained in [27]. It is based on classical principles of nonsmooth mechanics [28] and employs a time-stepping approach [29], which means impacts are resolved instantaneously without requiring contact parameters such as stiffness or damping.

The UR10 URDF file provided by the manufacturer is slightly adjusted to incorporate the real robot calibration and to include the force/torque sensor, gripper, and suction cup. This URDF file is used in experiments and simulations to define and control the robot. The carton boxes are modeled as fully rigid and arrive via the conveyor belt to the box alignment tool according to the pre-defined sequences.

[2]This work was partially supported by the Research Project I.AM. through the European Union H2020 program under GA 871899.

[3]See https://gitlab.tue.nl/robotics-lab-public/glue-application

[4]See `https://www.algoryx.se/partners-customers/` for a complete overview.

[5]See `https://www.algoryx.se/academia/`.

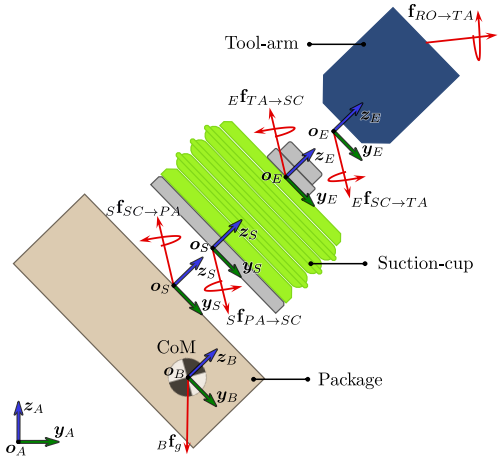


Fig. 5: Free Body Diagram of the bellows suction cup and package in a planar perspective. In the picture, ${}_{B}\mathbf{f}_{g}$ is the gravitational wrench acting on the center of mass frame of the package. ${}_{S}\mathbf{f}$ is the wrench acting on the package applied by the suction cup, and similarly for the other expressions.

**Contact description:** To properly model the contact interactions, we specify the contact parameters by assigning a material to the box and each element that the box can interact with, and we define a coefficient of friction and coefficient of restitution that describes that contact. The specific values for these coefficients are listed in Table I and are the result of a set of various experiments as described in [30]. Instead of using the default Box-Friction model in Algoryx, we use the more realistic, however, computationally heavier, Iterative Projected Cone Friction model[6], using a polygonized friction cone, in line with the work presented in [29].

**Suction cup modeling:** In [12], a 6D force-displacement model was validated which allows to accurately predict the suction cup's deformation during holding while carrying an object (of known mass, center of mass location, and inertia) as well as the interaction forces involved. In this work, we assume the inertial parameters of the payload to be known, although, in principle, we envision them to be estimated online with approaches that resemble [31], with the addition of the suction cup model. A schematic overview of the interaction forces acting on the system can be seen in Figure 5. The wrench acting on the package applied by the suction cup is modeled as a driven spring and a damper, hence, two effects are acting from the suction cup on the package as

$$ \mathbf{f} = \mathbf{f}_{SPRG}({}^{E}\mathbf{H}_{S}; \mathbf{K}) + \mathbf{f}_{DAMP}({}^{E}\mathbf{H}_{S}; {}^{S}\mathbf{v}_{E,S}; \mathbf{D}) \tag{2} $$

with $\mathbf{K}, \mathbf{D} \in \mathbb{R}^{6\times 6}$ the symmetric and positive (semi-)definite stiffness and damping matrices, respectively, ${}^{S}\mathbf{v}_{E,S}$ the twist between frames $E$ and $S$, and $\mathbf{f}$ the coordinates of a wrench (vector of forces and moments $\boldsymbol{f}, \boldsymbol{\tau} \in \mathbb{R}^3$) with respect to a given frame, indicated as $\mathbf{f} = \left[\boldsymbol{f}; \boldsymbol{\tau}\right] \in \mathbb{R}^6$. Assuming quasi-static movements of the gripper, we consider only the spring wrench which has been derived from a geometric potential energy function defined on all $\mathrm{SE}(3)$,

[6]See the *www.algoryx.se* website on Iterative Projected Cone Friction.

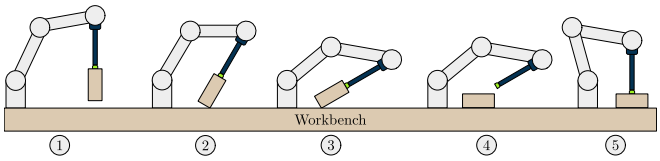


Fig. 6: The sequence of flipping a box. **1:** The robot approaches the workbench holding an item; **2:** The robot rotates the box around the edge of the item in contact with the workbench; **3:** The robot forces the item to rotate by sliding it on the workbench; **4:** The robot releases the item, and it comes to rest in a new orientation; **5:** The robot re-picks the item in this new orientation.

given as

$$\mathbf{f}_{SPRG} = -\frac{1}{4}\begin{bmatrix} {}^{S}\mathbf{R}_{S_1} & \mathbf{0}_{3\times3} \\ {}^{S}\mathbf{o}_{S_1}^{\wedge}\,{}^{S}\mathbf{R}_{S_1} & {}^{S}\mathbf{R}_{S_1} \end{bmatrix} \begin{bmatrix} \mathbf{R}^{\top}+\mathbf{I} & \mathbf{0}_{3\times3} \\ -(\mathbf{R}^{\top}\mathbf{o})^{\wedge} & (tr(\mathbf{R})\mathbf{I}-\mathbf{R}) \end{bmatrix} \mathbf{K} \begin{bmatrix} (\mathbf{R}^{\top}+\mathbf{I})\mathbf{o} \\ (\mathbf{R}-\mathbf{R}^{\top})^{\vee} \end{bmatrix}, \quad (3)$$

where we have used $\mathbf{H} = (\mathbf{R}, \mathbf{o})$ to indicate the local deformation ${}^{S_2}\mathbf{H}_{S_1} = ({}^{S_2}\mathbf{R}_{S_1}, {}^{S_2}\mathbf{o}_{S_1})$, with $S_1$ and $S_2$ defining the center of compliance, located between $E$ and $S$ (not shown in Figure 5). We thoroughly investigated the symmetry properties of the spring wrench model, leading to a simpler structure of the stiffness matrix and the identification procedure. The numerical values of the stiffness matrix have been identified, and the model validated, from a dataset containing 1200 static poses carrying objects with different masses and center of mass locations.

As an indication of the achievable pose prediction in steady state using the identified stiffness parameters, for an object of about 1.75 kg, we obtain a pose error in the order of 5 mm and 3°, with a gripper inclination of 60°. For further details about the suction cup model, we refer to [12]

**Control framework:** To control the robotic arm, we use the QP robot control software mc_rtc [32]. Within the control framework, we choose to use a Finite State Machine (FSM) to set up the controller. This FSM allows us to create a single controller that can be executed on various order sequences. Furthermore, this controller can communicate with both the simulation environment and the real robot without the need for any adjustments, allowing for a direct comparison between simulation and experiments. The controller is publicly available[7], allowing for reproducibility of the results.

**Motion primitives:** According to the sequences discussed in Section II, the boxes arrive on the conveyor and end up at the box-alignment tool, allowing the robot to pick them up. In practice, a packing algorithm provides the waypoints the robot follows to pick and place each item. As already discussed, we consider such an item-packing algorithm and motion planner as out of scope for this project. This means we choose and program the motion primitives for the items manually using the simulation environment. We will, however, try to mimic the behavior of a fictitious item-packing algorithm by following some guidelines:

- It cannot look ahead, i.e., there is no knowledge about the next incoming item but only of the item currently being processed and the items already placed in the container.
- Placement is permanent: once placed in the container, it cannot be re-picked and placed elsewhere.
- It can exploit the benefits of the developed suction cup model integrated into the simulation environment. For example, it may place items in tight spaces and use the compliance and modeling of the suction cup to its advantage, pushing the held item against other items already placed in the container.
- It may flip items around before placing by following a flip-repick-place sequence of motions. Figure 6 illustrates the sequence of motions that make the flipping of items possible.
- It will not place items in a potentially unstable manner inside the container. For example, if an item is so thin on one of its sides as to significantly increase the risk of tumbling over when placed on that side, the algorithm will prefer to flip the item around to place it on a more stable side.

The design of the motion primitives results in a set of waypoints, expressing the position and orientation of the control point of the robot arm (frame E in Figure 4), which we use for the Cartesian tasks in the QP-controller. For the trajectory planning between these waypoints, we follow the approach as discussed in [33, Chapter 5.6] and [34, Chapter 9]. The vacuum of the suction cup can be toggled at each waypoint, allowing the arm to pick up and release objects. For each sequence, the motion primitives and I/O controls are stored in CSV files, allowing the controller to easily switch between different sequences. These CSV files serve as input for the controller in both simulation and experiments.

## IV. Experimental testing

Figure 2 shows the experimental setup with the various components indicated, such as the robotic manipulator, gripper, suction cup, conveyor, and container. These components are representative of the type and size found in warehousing systems where pick-and-place robotic solutions operate. In detail, the setup contains the following equipment:

- A UR10 cobot equipped with a BOTA SenseONE EtherCat force torque sensor. Under it, a SmartRobotics GS002 vacuum gripper, with a Piab piGRIP 70mm diameter suction cup with a foam lip;
- A conveyor with a metal frame used to position the boxes on the conveyor for pick-up;
- A 570x370x250 mm container for item placement;
- A Zivid 2 3D vision camera, looking directly into the target container, capturing the state of the container after each box placement (not shown in Figure 2);
- An OptiTrack motion capture system setup consisting of 6 cameras, tracking the pose of each box, the gripper, the suction cup, and the container via unique patterns of passive reflective markers at 120FPS with sub-millimeter accuracy.

[7]See the code online: `www.github.com/MaartenJongeneel/FSM-Bin-Packing`

Fig. 7: Packing results as obtained from experiments (top row) and simulation (bottom row). Each column represents a different sequence.

Having obtained the motion primitives from Section III, we can now execute the controller on the real setup. To this end, we execute the following procedure for each item sequence:

1 The mc_rtc control application is started;
2 The next item arrives at the box aligner;
3 The robot picks the item from the pick-up point and places it in the target container according to the predefined motions as obtained from simulation;
4 The Zivid 2 camera takes a RGB and point cloud image to capture the state of the container;
5 Steps 2-4 are repeated until no more items can be placed or the full sequence has been completed;
6 The collected data from the robot's operation, the depth and RGB images of the target container, and from OptiTrack are stored for later analysis.

For each new sequence, we calibrate the force/torque sensor, after which we record each sequence three times to account for any uncertainties. For each recording, we collect data from the UR10 encoder and I/O output, the Zivid, the force/torque sensor, the mc_rtc control log, the motion capture system, and a video camera used to film the experiment for reference. The raw data files are then converted into an archive, according to the structure described in [35].

## V. Evaluating the Sim-to-Real Gap

The accuracy of the simulated model indicates if a future motion planner can use the predicted motions to reduce margins during item placement to increase stacking density. In this section, we analyze this accuracy based on various performance criteria, defined with a focus on the developed components and objectives. They are listed as follows:

1 **Execution**: It should be possible to execute the generated motion primitives and the complete sequences on the experimental setup, as in the simulation.
2 **Final Box poses**: The simulated rest positions and orientation of the boxes in the container should match those in experiments.
3 **Holding Box poses**: The simulated positions and orientations of the boxes during the holding phase with the suction gripper should match those in the experiments, indicating the fidelity of the suction cup model.
4 **Wrench predictions**: The simulated wrenches acting on the robot should match those in the experiments, indicating the fidelity of the robot and suction cup model implementation during complex contact phases inside the container.

The first criterion determines if the full sequence can be executed on the real setup as expected from the simulation. The second criterion defines to what extent the performed placement is as expected. Proper placement is crucial to prevent placed boxes from sticking out of the container, which can cause problems further down the industrial line. The third and fourth criteria focus on the fidelity of the suction cup model and the general implementation of the models into the physics engine. Such criteria evaluate the pose and wrench predictions and show to what extent those predictions can be used for trajectory planning and force feedback. We evaluate these last two criteria on carefully selected key motions from different sequences, whose execution is crucial to prevent the failure of packing boxes.

### A. Performance Validation

For each of the defined criteria, we will evaluate the performance in the five different sequences. It is worth noting that all experiments and simulations were executed in open-loop, i.e., once an algorithm has determined the box placement pose and the sequence of way-points to achieve this motion are generated, the sequence is executed without using any sensor feedback on object poses.

**Execution**: We applied the generated motion primitives on the real setup, and, remarkably, all motions executed properly. However, due to the non-modeled effects of the release phase of the suction cup, a systematic error occurred for each re-pick of a flipped box. In real experiments, the box is pushed a few centimeters away by the suction cup extending during release, which is not modeled in simulations. We account for this systematic error by adjusting the re-pick position in the controller without changing the motion primitives. Note that in industrial applications, vision feedback can determine the pose of the box, but this is out of scope in this work.

**Final Box Poses**: After running each of the sequences on the real-setup, the state of the boxes in the container was captured in order to compare to the final box's poses as obtained from simulation. In Figure 7, the final results of the boxes in the container are shown for the simulations (top row) and the experiments (bottom row), for each of the

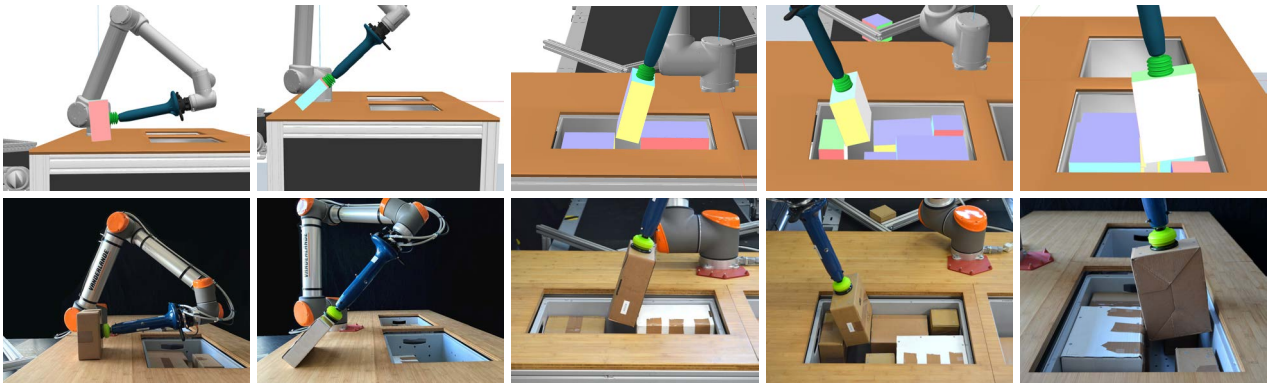

Fig. 8: Five of the selected key moments in simulation (top) and experiments (bottom) for the analysis of the pose and wrench predictions in the model. From left to right: Box016 in sequence 1, Box026 in sequence 2, Box028 in sequence 3, Box015 in sequence 4, and Box027 in sequence 5.

5 sequences. Furthermore, we have analyzed the pose error between the simulation and the experiments and compute the average position and orientation error according to

$$\bar{e}_{pos} = \frac{1}{N}\sum_{i=1}^{N} \left\| {}^{W}\mathbf{o}_{B}^{sim}(i) - {}^{W}\mathbf{o}_{B}^{exp}(i) \right\|, \tag{4}$$

$$\bar{e}_{rot} = \frac{1}{N}\sum_{i=1}^{N} \left\| \log\left( \left( {}^{W}\mathbf{R}_{B}^{exp}(i) \right)^{-1} {}^{W}\mathbf{R}_{B}^{sim}(i) \right) \right\|, \tag{5}$$

where $i$ is the box index and $N$ indicates the total number of boxes used in a sequence, and we have listed these errors in Table II. The simulation results show placement position errors almost always below one centimeter and placement orientation errors below two degrees, which is impressive given the complex movements of some of the boxes (e.g., the flipping motions).

**Box holding poses and wrenches**: In this section, we consider five motions of interest for further evaluation, shown in Figure 8. We discuss one of those motions in detail and refer to [36] for further analysis. The motion we consider concerns flipping and stacking Box016 in Sequence 1. In Figure 10, the left column shows the $x$-, $y$-, and $z$-components of the position vector, and the norm of the position error, while the right column shows the three components of the rotation vector and the norm of the rotation error over time. Similarly, Figure 11 shows the forces and the force error in the left column, while the right column shows the torques and the torque error. Both figures have the same time window, allowing for a direct comparison.

We consider a few moments of interest, also depicted in Figure 9. First, at $t = 129$ seconds, the box is picked up and rotated before being placed on the workbench. The position error along this motion is around 1.5cm, and the rotation error stays below $5°$. During the pick-up procedure, we observe an error in the $z$-component of the position at $t = 131$. This error comes from the unmodeled effect of the suction cup changing length due to a vacuum that appears as soon as it comes in contact with the box. At $t = 137$, the robot releases the box on the workbench. In the experiment, the vacuum turns off, and the suction cup elongates, pushing the box approximately 2cm away. This

TABLE II: Average position and orientation error of the final box poses in the container, together with the duration time of the sequence.

| | Seq.1 | Seq. 2 | Seq. 3 | Seq. 4 | Seq. 5 |
|---|---|---|---|---|---|
| $\bar{e}_{pos}$ [mm] | 6.60 | 9.68 | 7.52 | 9.26 | 10.08 |
| $\bar{e}_{rot}$ [deg] | 1.68 | 1.89 | 1.81 | 1.93 | 1.53 |
| Duration [s] | 253 | 236 | 296 | 277 | 290 |

unmodeled effect is visible in the position error and in the $y$-component of the position vector. This unmodeled release causes an orientation error of about $8°$. Recall that the F/T sensor is placed between the gripper and the robot's flange, meaning that its readings are affected by the gripper's mass. Although minor deviations occur, the simulation accurately captures the overall forces and torques measured during this motion, even with the inclusion of the suction cup model. At $t = 145$, the box is re-picked with a slight difference in location due to the unmodeled release phase, causing minor pose and wrench errors, which diminish in the 5 seconds after, as the robot's trajectories in experiments and simulation converge back to the same way-point at $t = 150$. From $t = 150$ till $t = 155$, the box is placed inside the container. At $t = 153$, the box slightly wobbles in simulation before coming to rest, causing a rapid orientation change not seen in the experiment, resulting in a mismatch in force and torque predictions. Since no feedback is used, the controller cannot compensate for this mismatch. However, the final position and orientation error at $t = 155$ is only 4.2 mm and $3.6°$, respectively. The RMS position and orientation norm errors resulting from the complete motion amount to 26.26 mm and $5.45°$, respectively, while the force and torque RMS error norms are 7.75 N and 1.08 Nm, respectively. We perform the same analysis for the other boxes across all sequences, with their resulting errors shown in Table III.

We run all simulations independent of the experiments. Since Box016 is the seventh box of sequence 1, minor deviations in the placement of previous boxes can lead to impacts in simulations that will not occur in experiments. In practice, pose-estimation methods can provide additional information to update the simulation scene. The resulting pose and wrench predictions show that the implemented physics models in Algoryx can accurately describe the different phenomena in the experiment, such as contacts, friction, restitution, and the suction-cup elastic behavior.

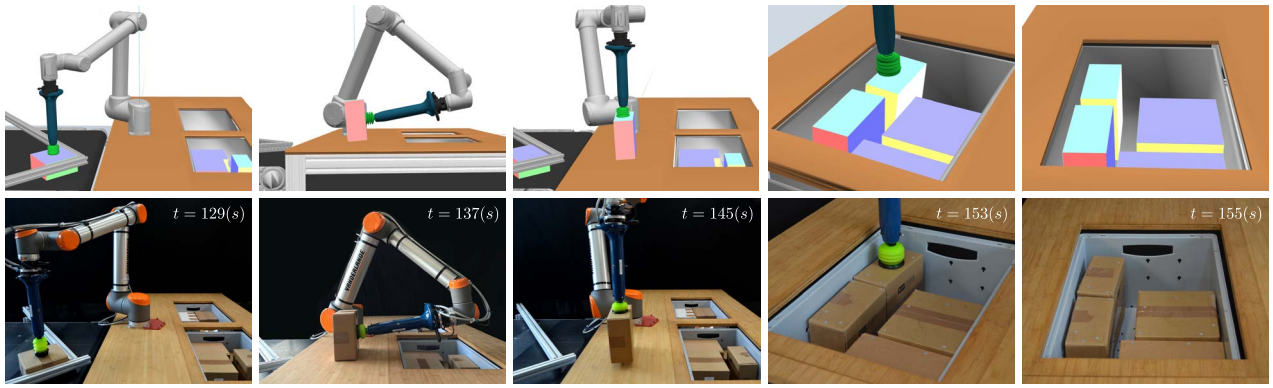


Fig. 9: Snapshots showing the flipping and stacking motion of Box016. At time $t = 129$, the box is picked up, rotated, and then placed at $t = 137$. It is picked up again at $t = 145$ and placed and released at $t = 153$, after which the robot moves away at $t = 155$.

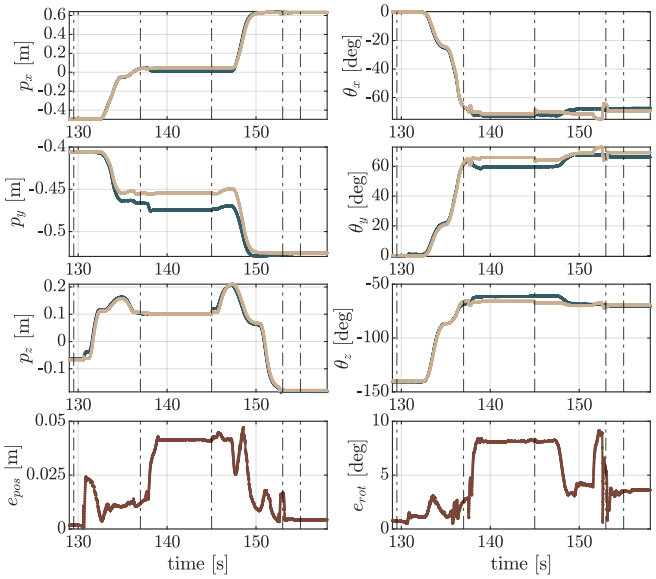


Fig. 10: Poses of Box016 obtained from experiments (—) and simulation (—), together with the error (—) for the motion of Figure 9.

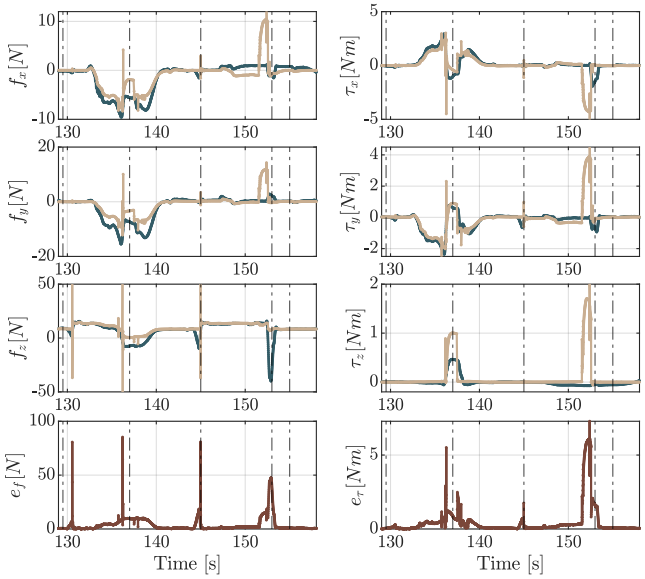


Fig. 11: Wrenches obtained from experiments (—) and simulation (—), together with the error (—) for the motion of Figure 9.

TABLE III: RMS values of the position, orientation, force, and torque errors for the five selected key motions. Each motion takes between 20-30 seconds.

| $RMS$ value | Seq.1 Box016 | Seq. 2 Box026 | Seq. 3 Box028 | Seq. 4 Box015 | Seq. 5 Box027 |
|---|---|---|---|---|---|
| Pos. [mm] | 26.26 | 24.09 | 59.72 | 24.52 | 28.21 |
| Rot. [deg] | 5.49 | 2.11 | 4.54 | 6.00 | 4.02 |
| Force [N] | 7.75 | 19.79 | 38.15 | 19.08 | 30.80 |
| Torque [Nm] | 1.08 | 0.89 | 0.78 | 1.15 | 0.99 |

These models can serve as a prior for trajectory planning, providing insight into expected impact events and allowing for advanced planning and manipulation control for robotic process automation for logistics operations.

**Comparison with state of the art:** In related work [13], directly computing the suction cup deformation and object poses leads to large errors. Instead, the authors determine the deformation based on the previous solution. Furthermore, their goal is slightly different than ours, aiming to tilt an object (while in contact with the environment) to a specific angle. In contrast, we *do* directly compute the suction cup deformation and object pose, resulting in errors in the order of 5mm and 3°, with a gripper inclination of 60° [12]. In [14], the authors consider the force in the longitudinal direction of the suction cup rather than the pose, reporting an average error of 2.1N while stating that accurately predicting the direction of deformation is virtually impossible. They assume that deformation and the resulting force are linearly dependent, which they state is not the case. Our employed model reports RMS errors of 0.69N and 0.067Nm over 608 experiments with masses up to 2.821 kg and tool-arm inclination angles up to 65°. Additionally, simulations using a rigid link instead of the model showed that tasks failed due to the inability of the simulation to handle robot-object-environment interactions. In future work, we aim to compare the performance of our simulation environment in RACK to commonly used frameworks such as Gazebo.

## VI. Conclusion and Future Work

Exploiting contacts between robots, objects, and environments benefits robotic manipulation tasks. In item-packing robotic applications, this approach allows robots to pack more items in the same container, which reduces transportation and operational costs compared to current robotic solutions, making the adoption of robots employing this technology more viable and financially appealing.

We use a rigid-body dynamics simulator to predict complex manipulation tasks using a vacuum gripper. These tasks involve flipping boxes and placing them into a container, as is relevant to the e-commerce industry. We consider densely filled objects, as objects with internal moving masses would require CoM position estimation using suction cups, which, to our knowledge, is currently unavailable as a technology. We validate the simulation environment on experimental data, reaching impressive levels of accuracy. The results show a good match between simulated and measured poses and wrenches during challenging multi-contact situations involving flipping and stacking boxes, thereby validating the suction cup model and its implementation in Algoryx.

These results motivate further research into contact-rich motion planning and packing algorithms and facilitate the adoption of industrial robotic applications in e-commerce, paving the way for advanced planning and manipulation control in robotic process automation for logistics operations.

## REFERENCES


[1] S. Ahmad, D. Sarwo Utomo, P. Dadhich, and P. Greening, "Packaging design, fill rate and road freight decarbonisation: A literature review and a future research agenda," *Cleaner Logistics and Supply Chain*, vol. 4, p. 100066, 2022.

[2] H. Xiong, K. Ding, W. Ding, J. Peng, and J. Xu, "Towards reliable robot packing system based on deep reinforcement learning," *Advanced Engineering Informatics*, vol. 57, p. 102028, 2023.

[3] Z. Zhou, Z. Zhang, K. Xie, X. Zhu, H. Huang, and Q. Cao, "A method of tight placement for robotic dense packing," in *2022 International Conference on Advanced Robotics and Mechatronics (ICARM)*, 2022, pp. 707–712.

[4] W. Shuai, Y. Gao, P. Wu, G. Cui, Q. Zhuang, R. Chen, and X. Chen, "Compliant-based robotic 3d bin packing with unavoidable uncertainties," *IET Control Theory & Applications*, vol. 17, no. 17, pp. 2241–2258, 2023.

[5] F. Wang and K. Hauser, "Dense robotic packing of irregular and novel 3d objects," *IEEE Transactions on Robotics*, vol. 38, no. 2, pp. 1160–1173, 2022.

[6] M. Agarwal, S. Biswas, C. Sarkar, S. Paul, and H. S. Paul, "Jampacker: An efficient and reliable robotic bin packing system for cuboid objects," *IEEE Robotics and Automation Letters*, vol. 6, no. 2, pp. 319–326, 2021.

[7] R. Shome, W. N. Tang, C. Song, C. Mitash, H. Kourtev, J. Yu, A. Boularias, and K. E. Bekris, "Towards robust product packing with a minimalistic end-effector," in *2019 International Conference on Robotics and Automation (ICRA)*, 2019, pp. 9007–9013.

[8] J. F. Gonçalves and M. G. Resende, "A biased random key genetic algorithm for 2d and 3d bin packing problems," *International Journal of Production Economics*, vol. 145, no. 2, pp. 500–510, 2013.

[9] F. Gabriel, M. Fahning, J. Meiners, F. Dietrich, and K. Dröder, "Modeling of vacuum grippers for the design of energy efficient vacuum-based handling processes," *Production Engineering*, vol. 14, no. 5, pp. 545–554, Dec 2020.

[10] J. Mahler, M. Matl, X. Liu, A. Li, D. Gealy, and K. Goldberg, "Dex-Net 3.0: Computing Robust Vacuum Suction Grasp Targets in Point Clouds Using a New Analytic Model and Deep Learning," in *2018 IEEE International Conference on Robotics and Automation (ICRA)*, 2018, pp. 5620–5627.

[11] K.-T. Yu and A. Rodriguez, "Realtime state estimation with tactile and visual sensing for inserting a suction-held object," in *2018 IEEE/RSJ International Conference on Intelligent Robots and Systems (IROS)*, 2018, pp. 1628–1635.

[12] A. A. Oliva, M. J. Jongeneel, and A. Saccon, "A compact 6D suction cup model for robotic manipulation via symmetry reduction," *Submitted to: IEEE Transactions on Robotics (T-RO)*, Mar 2024.

[13] X. Cheng, Y. Hou, and M. T. Mason, "Manipulation with Suction Cups Using External Contacts," in *Robotics Research*. Cham: Springer International Publishing, 2022, pp. 692–708. [Online]. Available: https://doi.org/10.1007/978-3-030-95459-8_42

[14] J. Hudoklin, S. Seo, M. Kang, H. Seong, A. T. Luong, and H. Moon, "Vacuum suction cup modeling for evaluation of sealing and real-time simulation," *IEEE Robotics and Automation Letters*, vol. 7, no. 2, pp. 3616–3623, 2022.

[15] Algoryx Simulation AB, "AGX Dynamics," Umeå, Sweden, 2022, version 2.30.0.0. [Online]. Available: https://www.algoryx.se/agx-dynamics/

[16] "TU/e Impact-Aware Robotics Database," Eindhoven, The Netherlands, 2022, accessed: 2024-04-22. [Online]. Available: https://impact-aware-robotics-database.tue.nl/

[17] A. Zermane, N. Dehio, and A. Kheddar, "Planning impact-driven logistic tasks," *IEEE Robotics and Automation Letters*, vol. 9, no. 3, pp. 2184–2191, 2024.

[18] C. Pezzato, "Exploring active inference and model predictive path integral control: A journey from low-level commands to task and motion planning," Dissertation (TU Delft), Delft University of Technology, 2024.

[19] G. Williams, P. Drews, B. Goldfain, J. M. Rehg, and E. A. Theodorou, "Information-theoretic model predictive control: Theory and applications to autonomous driving," *IEEE Transactions on Robotics*, vol. 34, no. 6, pp. 1603–1622, 2018.

[20] S. Traversaro and A. Saccon, *Multibody dynamics notation (version 2)*. Technische Universiteit Eindhoven, Nov. 2019, DC2019.100.

[21] P. Gergondet, C. Lacoursière, F. Nordfeldth, and J. van Steen, "Deliverable D1.2: Physics Engine API for Learning, Planning, Sensing, and Control," H2020 EU Project I.AM. Consortium, Tech. Rep. D1.2, Nov. 2023.

[22] M. Cao, K. Cao, S. Yuan, T.-M. Nguyen, and L. Xie, "Neptune: Nonentangling trajectory planning for multiple tethered unmanned vehicles," *IEEE Transactions on Robotics*, pp. 1–19, 2023.

[23] V. Wiberg, E. Wallin, M. Servin, and T. Nordfjell, "Control of rough terrain vehicles using deep reinforcement learning," *IEEE Robotics and Automation Letters*, vol. 7, no. 1, pp. 390–397, 2022.

[24] J. Styrud, M. Iovino, M. Norrlöf, M. Björkman, and C. Smith, "Combining planning and learning of behavior trees for robotic assembly," in *2022 International Conference on Robotics and Automation (ICRA)*, 2022, pp. 11 511–11 517.

[25] G. Li, H. B. Waldum, M. O. Grindvik, R. S. Jørundl, and H. Zhang, "Development of a vision-based target exploration system for snake-like robots in structured environments," *International Journal of Advanced Robotic Systems*, vol. 17, no. 4, 2020.

[26] M. Omer, K. Merckaert, B. Vanderborght, and G. van de Perre, "Constraint control for non-prehensile robotic transportation," in *43rd Benelux Meeting on Systems and Control*, 2024.

[27] C. Lacoursière, "Ghosts and machines : regularized variational methods for interactive simulations of multibodies with dry frictional contacts," Ph.D. dissertation, Umeå University, Computing Science, 2007.

[28] B. Brogliato, *Nonsmooth Mechanics*, 3rd ed. Springer International Publishing Switzerland, 2016.

[29] D. Stewart and J. C. Trinkle, "An Implicit Time-Stepping Scheme for Rigid Body Dynamics with Inelastic Collisions and Coulomb Friction," *International Journal for Numerical Methods in Engineering*, vol. 39, no. 15, pp. 2673–2691, 1996.

[30] C. F. Henst, "Quantifying the Sim-to-Real Gap in Robotic Bin Packing via Nonsmooth Physics Simulation," Master's thesis, Eindhoven University of Technology, Faculty of Mechanical Engineering, Dynamics and Control Group, February 2024, DC 2024.010.

[31] A. Kurdas, M. Hamad, J. Vorndamme, N. Mansfeld, S. Abdolshah, and S. Haddadin, "Online payload identification for tactile robots using the momentum observer," in *2022 International Conference on Robotics and Automation (ICRA)*, 2022, pp. 5953–5959.

[32] CNRS-AIST JRL, CNRS LIRMM, "mc_rtc," 2020. [Online]. Available: https://jrl-umi3218.github.io/mc_rtc/index.html

[33] M. W. Spong, S. Hutchinson, and M. Vidyasagar, *Robot modeling and control*. John Wiley & Sons, 2006.

[34] K. M. Lynch and F. C. Park, *Modern Robotics: Mechanics, Planning, and Control*, 1st ed. USA: Cambridge University Press, 2017.

[35] M. J. Jongeneel, S. Dingemans, and A. Saccon, "The Impact-Aware Robotics Database: Supporting Research Targeting the Exploitation of Dynamic Contact Transitions," *Submitted to: IEEE Robotics and Automation Letters (RA-L)*, August 2023.

[36] R. Duarte, S. Eisinger, M. Jongeneel, F. Nordfeldth, and A. Oliva, "Deliverable D5.4: Scenario 2 (BOX) report," H2020 EU Project I.AM. Consortium, Tech. Rep. D5.4, 2024.